IEEE Access
Multidisciplinary | Rapid Review | Open Access Journal

SPECIAL SECTION ON INTELLIGENT DATA SENSING, COLLECTION AND DISSEMINATION IN MOBILE COMPUTING

Received May 24, 2019, accepted June 18, 2019, date of publication July 26, 2019, date of current version November 14, 2019.

Digital Object Identifier 10.1109/ACCESS.2019.2931459

Joint Communication and Control for Small Underactuated USV Based on Mobile Computing Technology

TINGTING YANG[1,2], (Member, IEEE), YUEJUN GUO[2], YI ZHOU[3], (Member, IEEE), AND SIWEN WEI[2]

[1]School of Electrical Engineering and Intelligentization, Dongguan University of Technology, Dongguan 523000, China
[2]Navigation College, Dalian Maritime University, Dalian 116026, China
[3]School of Computer and Information Engineering, Henan University, Kaifeng 475004, China

Corresponding author: Yi Zhou (zhouyi@henu.edu.cn)

This work was supported in part by Natural Science Foundation of China under Grant 61771086, Dalian Outstanding Young Science and Technology Talents Foundation under Grant 2017RJ06, Dalian High-Level Innovative Talent Project under Grant 2016RQ035, Liaoning Province Xingliao Talents Program under Grant XLYC1807149, Equipment Pre-Research Fund Project under Grant 61403120402, Open Research Project of the State Key Laboratory of Industrial Control Technology, Zhejiang University, China, under Grant ICT1900314.

ABSTRACT To satisfy the requirement of the future ocean communication and maritime transportation, in this paper, an integrated space–air–ground–sea communication control system based on mobile computing technology is proposed to rescue a water container. Specifically, unmanned surface vehicle (USV), as a flexible and lightweight intelligent device deployment integration platform, is the main tool to move towards the water container. However, how to sense the real-time navigation status information of the USV, integrate the information, and eventually distribute it to the ground control center, is still a difficult point for us. To successfully rescue the water container, three aspects of research are needed: information collection of the USV, information fusion, and data distribution to the ground control center. For the information collection part, we mainly use nine-axis, ultrasonic, global positioning system (GPS), and ultra wide band (UWB) sensors to complete the information collection for the USV. For the information fusion part, we set up a computational model to solve it. The USV computational model in previous works is mainly based on large ships, ignoring the modeling of wind, wave, and current for small underactuated USV. We use the classical Nomoto model, combined with the actual any slight wind, wave, and current forces on the USV, and finally combined with the proportion integration differentiation (PID) algorithm to model the USV. For the data distribution to the ground control center part, we have set up a communication protocol for the USV so that it can communicate normally. In addition, we wrote a Browser/Server (B/S) architecture to enable the ground control center to communicate with the host computer. Finally, our proposed control and communication schemes are carried out on actual USV. The real experiments show that the proposed schemes can reduce the ship surge and satisfy the ship navigation.

INDEX TERMS Information collection, computational model, USV, data distribution, space-air-ground-sea integration.

I. INTRODUCTION

The 21st century is the century of the ocean. The ocean is rich in biological resources, oil and gas resources and mineral resources. It is a strategic space and resource for human survival and sustainable development [1]. To better understand, develop and protect the ocean, unmanned surface vehicle (USV) has been widely applied in many ocean activities. In the military field, USV can be used for intelligence gathering, anti-mine warfare, anti-submarine warfare, special forces operations, electronic warfare, and maritime interception operations [2]. In the civilian field, USV can be used for marine environmental monitoring, hydrographic surveys, maritime search and rescue, and ship replenishment,

The associate editor coordinating the review of this manuscript and approving it for publication was Anfeng Liu.

which not only ensure the safety of personnel, but also greatly improve the efficiency of operations [3]. Therefore, USV technology has become the focus of researchers at home and abroad.

In the 1990s, the US Navy developed the USV for automatic search, detection, and automatic monitoring at sea and developed a networked remote control sea area security system [4]. The unmanned sea exploration vessel "Tianxiang No.1" developed by Shenyang Xinguang Company in China was successfully applied to the meteorological service guarantee work of Qingdao Olympic Sailing during the Beijing Olympic Games [5]. In 2009, Tianjin University cooperated with the National Ocean Technology Center in the 863 project to launch a small underwater autonomous observation platform [6]. The underwater intelligent robot laboratory of Harbin Engineering University completed the design and construction of a certain type of unmanned boat, and carried out related technical research and sea trials [7]. The fully automatic unmanned ship developed by Zhuhai Yunzhou Intelligent Technology, Ltd. has formed a series of products and promoted it throughout the country [8].

At present, the research on USV focuse on various types of underwater robots and various types of medium and small remote control USV, which are mainly used in light applications such as marine survey, monitoring, measurement, and military applications [9]. The research areas of USV are ranging from hull design, path planning navigation, surface object detection and self-identification, obstacle avoidance, to motion control [10]. It covers a wide range of technical fields, including hydrodynamics, autonomous decision-making, automatic control, signal processing, networ communication, sensor technology, etc [11], [12]. In many key technology fields of USV, their basic research problems are the path control and communication protocol of USV. However, how to sense the real-time navigation status information of the ship in the ground control center and fuse the information to better complete the control of the USV remotely is still a difficult point for us. Mobile computing technology can enable computers or other information intelligent terminal devices to achieve data transmission and resource sharing in a wireless environment [13]. It just solved the above problems. Its role is to provide useful, accurate and timely information to any customer, anytime, anywhere. This coincides with the problems we have encountered. We verify the correctness of the computational model and communication protocol in the context of the location at the designated container. In this paper, aiming at the mobile computing technology, an integrated Space-Air-Ground-Sea communication control system for USV is proposed to solve a series of practical problems such as information coverage at sea, searching and positioning, under which the motion model and communication protocol of USV are designed. The main contributions are summarized as follows:

(1) In view of the heterogeneity of maritime communication, an Space-Air-Ground-Sea integrated communication control architecture based on mobile computing technology is proposed;

(2) The underactuated USV as the research object, based on the theory of hydrodynamics and mobile computing, introducing sensor data, combining with the Proportion Integration Differentiation (PID) algorithm, a computational model suitable for the USV is proposed.

(3) A communication protocol for communication between the ship control board and the host is designed on the USV. The Browser/Server (B/S) architecture is designed to realize the information dissemination and control instruction decoupling, and remotely monitor the USV.

(4) Real experiments are carried out in the container search and rescue scenarios. The ground control center controls the USV to the position of the container delivered by the underwater sensor. The drone monitors the condition of the ship in real time and transmits the information to the ground control center. The ground control center sends the corresponding command to the USV.

The reminder of this paper is organized as follows. Section II introduces the whole system model and design of Space-Air-Ground-Sea. Section III describes the algorithms used in the overall system and the problems encountered. Section IV proposes a system control model for the small USV on the unmanned surface ship's side for the problem of the third section. Section V shows the actual ship operation effect of the model. Section VI summarizes this article.

II. SPACE-AIR-GROUND-SEA INTEGRATED SYSTEM MODEL

A. OVERALL SPACE-AIR-GROUND-SEA STRUCTURE

As shown in Fig. 1, this paper designs an integrated Space-Air-Ground-Sea communication control system for USV based on mobile computing technology to solve a series of practical problems such as information coverage at sea, searching and positioning. With the background of container search and rescue work, the overall scenario of the small USV communication and control integrated system is as follows: the underwater sensor node transmits the information to the lead USV by sensing the position information of the container. After receiving the message, the lead USV dissemination the information to the ground control center through the wireless bridge. After receiving the information, the center disseminates an instruction to the lead USV to arrive at the location. After the lead USV receives the instruction, it disseminates the information to the sub USV which is closest to the container so that it can reach the designated location. During the operation, the drone monitors the corresponding sub ship, records the navigation status in real time, transmits it to the ground control center through the cloud server, and the USV also transmits the basic information such as the state and heading of the ship to the ground control center through the cloud server.

In Fig. 1, the integrated communication and control system based on mobile computing technology is composed of three parts: remote module of ground control terminal, the USV

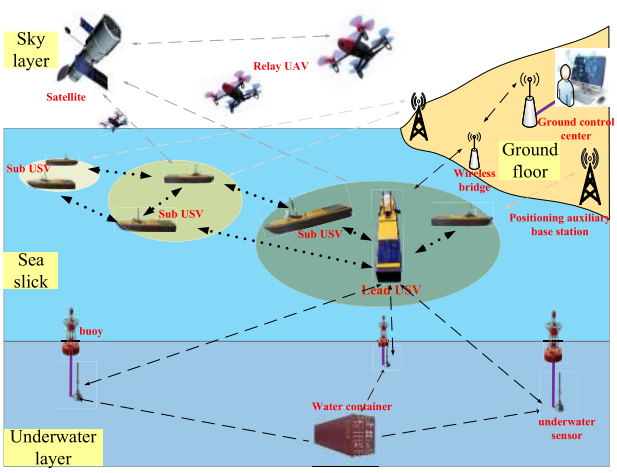

FIGURE 1. The overall structure of the system.

terminal module and the drone. Among them, the ground control terminal remote module mainly realizes the control and communication between the ground control center terminal and the USV. The USV terminal module mainly realizes the functions of data acquisition in the actual navigation process, instrument state control in the aircraft, time sequence control and cooperative operation with other sensors on the USV platform (such as GPS, UWB, nine-axis, etc.). The drone is mainly responsible for monitoring the operating state of the USV. Among these three parts, we propose a new system model for the small USV that is suitable for the computational model. Meanwhile we achieved a better route fit by GPS and UWB dual positioning. At the same time, the real-time communication transmission task requirement between the sensors is satisfied, and the remote control can be realized through the B/S architecture.

B. OVERALL STRUCTURE OF SHIP INTELLIGENT DATA SENSING

The data sensing design of this system is mainly focuses on the design of the USV terminal. It can be divided into three parts, namely the information collection part, the main control board part and the power supply part. The information collection includes five parts, namely attitude sensor (JY901), GPS (ATK-S1216F8), UWB (SWM1000), ZigBee (DRF1609), and ultrasonic (JSN-SR04T) modules. The main control board selects ATmega16. The power section has 5V, 3.7V and 12V. Its overall framework is shown in Fig. 2.

In Fig. 2, the information collection module senses data through sensors and disseminates data to USV host. The ship control panel controls the collection of basic data, such as battery power, cabin drainage, motor speed, steering angle, etc. The information between the ship control panel and the USV host is disseminated through the USB serial line. We design the transfer protocol between them, and then collect information through the host, and communicated with the ship control panel to make the ship run normally.

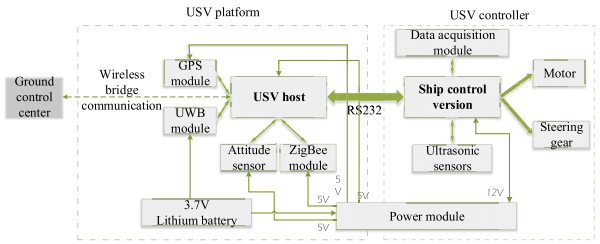

FIGURE 2. Structure diagram of USV terminal control system.

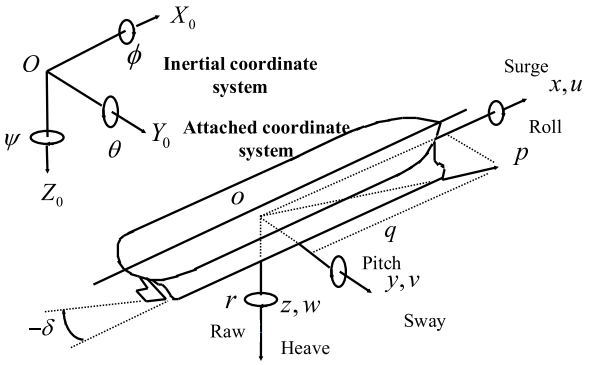

FIGURE 3. Reference coordinate system.

C. FLOW CHART OF USV TERMINAL SOFTWARE PROGRAM

The software design of the system mainly includes the information communication part between the ground control center and the ship control panel, the communication part between the ship control panel and the USV host, the communication part between the sensor and the USV host, and the information fusion part between the serial ports. The overall software operation is shown as Algorithm 1.

In Algorithm 1, the USV receiving information from the ground is constantly being updated. Therefore, in this system, if the ground control center does not send a stop command to the USV, the USV will always follow the straight line.

III. COMPUTATIONAL MODEL THEORY AND COMMUNICATION PROTOCOL

A. DYNAMICS COMPUTATIONAL ALGORITHM

The actual computational of the ship is extremely complex, with six degrees of freedom in general, including movements following three axes and rotation around three axes [14]. We use the two coordinate systems of the inertial coordinate system (the geodetic coordinate system) and the attached coordinate system to describe, and all follow the rule of the right-handed coordinate system. In the geodetic coordinate system, we care about the three position coordinates of the ship and three attitude angles, a total of six. In the attached coordinate system, we care about the ship's three translation speeds and three corner speeds, which are also six quantities [15]. As shown in Fig. 3, it is reference coordinate system.

Algorithm 1 Structure Diagram of USV Terminal Control System

```
Initialize the web page file and start the web page.
Serial port initialization.
while 1 do
  prevent step counts = prevent step counts +1
  Sensor data acquisition and data analysis
  while prevent step counts ≤ 5 do
    Calculate the course angle at this moment and set it as
    the initial course angle.
  end while
  Calculate the heading deviation at this time.
  Bring the course angle into the system model to get the
  rudder angle value.
  The motor is turned on and the ship moves straight
  ahead.
  if The ground control center sent a motion command =
  1 then
    Send to the straight by the sub ship.
  else if The ground control center sent a motion command
  = 2 then
    Sent to the designated location by sub ship.
    if Distance from the target point ≤ turning radius
    then
      rudder angle = 0 or rudder angle = 1000
    end if
    if Calculate the heading deviation ≥ 87 and Calculate
    the heading deviation ≤ 93 then
      rudder angle = 500
    end if
  else if The ground control center sent a motion command
  = 3 then
    Sending obstacles to the sub ship.
    if Front obstacle ≤ 1m then
      USV motor reversal 3s.
      the left full rudder is 2s.
    end if
    while Right full rudder = the previous heading do
      USV motor reversal 3s.
      the left full rudder is 2s.
    end while
  else
    Turn off the motor.
  end if
end while
```

The origin of the inertial coordinate system can be set at any position on the surface of the earth to describe the pose information of the USV, and the Newton's kinematic law is satisfied in this coordinate system. Generally, the center of gravity of the USV is selected as the origin of the hull coordinate system, which is used to describe the speed and force information of the USV. Among them, surging, swaying and heaving move around X axis, Y axis and Z axis respectively, while rolling, pitching and yawing rotate around X axis, Y axis and Z axis [16]. Table 1 shows the motion parameters of the USV.

TABLE 1. Motion parameters of USV.

Degree of freedom	Speed	Position and Euler Angle	Force
Surge	u	x	X
Sway	v	y	Y
Heave	w	z	Z
Roll	p	φ	K
Pitch	q	θ	M
Raw	r	ψ	N

In the actual small USV, we only consider three degrees of freedom which are surging, swaying and rawing. The basic equations of motion for these three degrees of freedom are given below [17]–[19]. Basic equation of ship plane motion (conventional Newtonian equation of motion):

$$\left.\begin{array}{l} m\left(\dot{u}-vr-x_c r^2\right)=X \\ m\left(\dot{v}-ur-x_c\dot{r}\right)=Y \\ I_{zz}\dot{r}+mx_c\left(\dot{v}+ur\right)=N \end{array}\right\}. \tag{1}$$

Hydrodynamic equation:

$$\begin{cases} X=X_u\Delta u+X_{\dot{u}}\dot{u} \\ Y=Y_v v+Y_r r+Y_{\dot{v}}\dot{v}+Y_{\dot{r}}\dot{r}+Y_\delta\delta \\ N=N_v v+N_r r+N_{\dot{v}}\dot{v}+N_{\dot{r}}\dot{r}+N_\delta\delta. \end{cases} \tag{2}$$

where $Y_v, Y_r, N_v, N_r, Y_{\dot{v}}, Y_{\dot{r}}, N_{\dot{v}}, N_{\dot{r}}, Y_\delta, N_\delta$ are 10 hydrodynamic derivatives, the equation is:

$$\begin{cases} Y'_v=-[1+0.40C_bB/T]\cdot\pi(T/L)^2-\gamma Y'_\delta \\ Y'_{\dot{v}}=-[1+0.16C_bB/T-5.1(B/L)^2]\cdot\pi(T/L)^2 \\ Y'_r=-[-0.5+2.2B/L-0.080B/T]\cdot\pi(T/L)^2 \\ \quad+\frac{1}{2}\gamma Y'_\delta,\ \gamma=0.30 \\ Y'_{\dot{r}}=-[0.67B/L-0.0033(B/T)^2]\cdot\pi(T/L)^2 \\ N'_v=-[0.5+2.4T/L]\cdot\pi(T/L)^2+\frac{1}{2}\gamma Y'_\delta \\ N'_{\dot{v}}=-[1.1B/L-0.041B/T]\cdot\pi(T/L)^2 \\ N'_{\dot{r}}=-[0.0833+0.017C_bB/T-0.33B/L]\cdot\pi(T/L)^2 \\ Y'_\delta=3.0A_\delta/L^2 \\ N'_r=-[0.25+0.039B/T-0.56B/L]\cdot\pi(T/L)^2 \\ \quad+\frac{1}{4}\gamma Y'_\delta,\ \gamma=0.30 \\ N'_\delta=-(1/2)Y'_\delta. \end{cases} \tag{3}$$

where B, T, C_b, A_δ are the ship width, draft, square factor, and rudder blade area respectively.

Combining the equations of Eq.(1) and Eq.(2), the linear equation of ship maneuvering motion is expressed in matrix form:

$$\begin{bmatrix} (m-Y_{\dot{v}}) & (mx_c-Y_{\dot{r}}) \\ (mx_c-N_{\dot{v}}) & (I_{zz}-N_{\dot{r}}) \end{bmatrix}\begin{bmatrix}\dot{v}\\ \dot{r}\end{bmatrix} = \begin{bmatrix} Y_v & (Y_r-mu_0) \\ N_v & (N_r-mx_cu_0) \end{bmatrix}\begin{bmatrix}v\\ r\end{bmatrix}+\begin{bmatrix}Y_\delta\\ N_\delta\end{bmatrix}\delta, \tag{4}$$

In the Eq.(4), the first row is divided by $\frac{1}{2}\rho L^3$ both ends, and the second row is divided by $\frac{1}{2}\rho L^4$ and converted into a

dimensionless hydrodynamic derivative:

$$\begin{bmatrix} m'-Y'_{\dot v} & L(m'x'_c-Y'_{\dot r}) \\ m'x'_c-N'_{\dot v} & L(I'_{zz}-N'_{\dot r}) \end{bmatrix}\begin{bmatrix}\dot v\\ \dot r\end{bmatrix} = \begin{bmatrix} \frac{V}{L}Y'_v & V(Y'_r-m') \\ \frac{V}{L}N'_v & V(N'_r-m'x'_c) \end{bmatrix}\begin{bmatrix} v\\ r\end{bmatrix}+\begin{bmatrix}\frac{V^2}{L}Y'_\delta\\ \frac{V^2}{L}N'_\delta\end{bmatrix}\delta, \tag{5}$$

The above equation can be abbreviated as:

$$I'_{(2)}\dot X_{(2)} = P'_{(2)}X_{(2)} + Q'_{(2)}U. \tag{6}$$

where $I'_{(2)}, P'_{(2)}, Q'_{(2)}$ are the inertial force derivative matrix, the viscous force derivative matrix, and the rudder force derivative matrix respectively, $X_{(2)} = \begin{bmatrix} v & r\end{bmatrix}^T$ is the state vector, and $U=\delta$ is the control input. Transform Eq.(6) into a standard state space form

$$\dot X_{(2)} = A_{(2)}X_{(2)} + B_{(2)}\delta. \tag{7}$$

In the above equation:

$$A_{(2)} = (I'_{(2)})^{-1}P'_{(2)} = \begin{bmatrix} a_{11} & a_{12}\\ a_{21} & a_{22}\end{bmatrix},$$
$$B_{(2)} = (I'_{(2)})^{-1}Q'_{(2)} = \begin{bmatrix} b_{11}\\ b_{21}\end{bmatrix}, \tag{8}$$

$$\begin{cases} a_{11} = [(I'_{zz}-N'_{\dot r})Y'_v - (m'x'_c - Y'_{\dot r})N'_v]V/S_1\\ a_{12} = \left((I'_{zz}-N'_{\dot r})(Y'_r-m')LV/S_1\right) - \\ \left((m'x'_c - Y'_{\dot r})(N'_r - m'x'_c)LV/S_1\right)\\ a_{21} = [-(m'x'_c - N'_{\dot v})Y'_v + (m'-Y'_{\dot v})N'_v]V/L/S_1\\ a_{22} = -\left((m'x'_c - N'_{\dot v})(Y'_r-m')/S_1\right) + \\ \left((m'-Y'_{\dot v})(N'_r - m'x'_c)V/S_1\right)\\ b_{11} = [(I'_{zz}-N'_{\dot r})Y'_\delta - (m'x'_c - Y'_{\dot r})N'_\delta]V^2/S_1\\ b_{21} = [-(m'x'_c - N'_{\dot v})Y'_\delta + (m'-Y'_{\dot v})N'_\delta]V^2/L/S_1\\ S_1 = \left((I'_{zz}-N'_{\dot r})(m'-Y'_{\dot v})L\right) - \\ \left((m'x'_c - N'_{\dot v})(m'x'_c - Y'_{\dot r})L\right). \end{cases} \tag{9}$$

Nomoto has done an excellent simplification of the Eq.(6) ship computational model to reduce it to second order. The starting point of the argument is that for ships with such large inertia, the dynamics are only important in the low frequency range, let $s = j\omega \to 0$, and use a well-known approximation [20]:

When $x \to 0$, there is $(1-x) \approx 1/(1+x)$, and the 2nd and 3rd order small quantities are ignored, thus derive the famous Nomoto model [21]:

$$G_{\psi\delta}(s) = \frac{\psi}{\delta} = \frac{K_0}{s(T_0 s+1)}, \tag{10}$$

In the above equation:

$$K_0 = \frac{b_{11}a_{21} - b_{21}a_{11}}{a_{11}a_{22} - a_{12}a_{21}}, \tag{11}$$

$$T_0 = -\frac{a_{11}+a_{22}}{a_{11}a_{22}-a_{12}a_{21}} - \frac{b_{21}}{b_{11}a_{21}-b_{21}a_{11}}. \tag{12}$$

In Eq.(10), it is a linear model, but in practice, when used in the simulation study of closed-loop control systems of ships, the dynamic characteristics of the controlled process must be expressed in a nonlinear model, and environmental disturbances caused by wind, waves and currents must also be considered. The right end of the two-degree-of-freedom equation is added with a nonlinear hydrodynamic term, a wind term, and a wave term. Then the dimensionless two-degree-of-freedom nonlinear ship computational model will take the following form [22]:

$$I'_{(2)}\dot X_{(2)} = P'_{(2)}X_{(2)} + Q'_{(2)}U + F'_{NON} + F'_{WIND} + F'_{WAVE}, \tag{13}$$

where $F'_{NON}, F'_{WIND}, F'_{WAVE}$ is the force of the wind and the current on the ship, its expression is as follows:

$$F'_{NON} = \begin{bmatrix} Y_{NON}\Big/\frac{1}{2}\rho L^3\\ N_{NON}\Big/\frac{1}{2}\rho L^4\end{bmatrix},$$
$$F'_{WIND} = \begin{bmatrix} Y_{WIND}\Big/\frac{1}{2}\rho L^3\\ N_{WIND}\Big/\frac{1}{2}\rho L^4\end{bmatrix},$$
$$F'_{WAVE} = \begin{bmatrix} Y_{WAVE}\Big/\frac{1}{2}\rho L^3\\ N_{WAVE}\Big/\frac{1}{2}\rho L^4\end{bmatrix}. \tag{14}$$

where $Y_{NON}, Y_{WIND}, Y_{WAVE}$ and$N_{NON}, N_{WIND}, N_{WAVE}$ are the resultant forces of the non-linear force, wind force and wave force in the y direction and the resultant moments around the z axis respectively.

But we have a lot of problems with the practical application of this computational model: In this nonlinear model, the nonlinear hydrodynamic, wind, and wave terms are not tested in practice and cannot be applied to unmanned ships. At the same time, the computational model is a model for large ships and cannot be used in small USVs. Therefore, it is urgent to propose a ship computational model that is suitable for a small USV. In the fourth section we have elaborated on the improved ship computational model.

B. TRACK TRACKING

In the course of route tracking, firstly we need to make the USV reach a specified location. The idea is setting the latitude and longitude of the destination to the destination point, and calculating the starting heading angle to the destination point, which is the setting heading angle. Start straight-line driving, collect the heading value of the nine-axis transmission on the way, and calculate the distance between the actual ship and the set point. If the heading deviates from the original orbit and the distance suddenly increases, calculate the heading value of the latitude and longitude and the destination point measured by GPS at this moment, and then adjust accordingly until the specified point is reached.

1) HEADING ANGLE CALCULATION

In the calculation of the heading angle, three methods are summarized by consulting for information:

The first is the spherical sine equation. This method can theoretically be used to calculate the heading between any two points on the earth. However, this method uses the cosine of the spherical sine equation and has higher requirements for the accuracy of the system floating point [23].

The second is the plane rectangular coordinate system method. The basic idea of this method is to convert the longitude difference and the latitude difference into the ground distance and then use the plane geometry knowledge to solve. Therefore, it can only be used for short-distance calculation where the mid-latitude area is below 40km. Because the calculation is simpler, it is relatively advantageous [24].

The third is the polar coordinate method. The method can be used to calculate the heading between any two points on the earth. Its idea is to put the earth in a spherical coordinate system and adjust the starting point of the three parameters to reduce the amount of calculations later, then convert each point from spherical coordinates to rectangular coordinates, and then obtain the The angle between the two sides that is also the heading according to the theorem of plane normal vector. Finally convert it to the degree that conforms to the heading definition [25], [26].

In view of the above three aspects, we choose the third method to solve the heading angle. The method is elaborated below:

The latitude and longitude of two points A and B are $A(Aj, Aw)$ and $B(Bj, Bw)$. Define three temporary variables x, y, A before calculating:

$$\begin{aligned} x &= \sin(Bj - Aj)\cos(Bw) \\ y &= \cos(Aw)\sin(Bw) - \sin(Aw)\cos(Bw)\cos(Bj - Aj), \end{aligned} \quad (15)$$

Substitute the value obtained x, y into the following function:

$$A = a\tan 2(x, y), \quad (16)$$

The function $a\tan 2$ is a set of methods for converting rectangular coordinates into polar coordinates.

After getting A, take it to the next step, and the *MOD* function asks for the remainder:

$$Beaning = MOD(A, 360). \quad (17)$$

The desired *Beaning* is the desired heading value.

2) DISTANCE CALCULATION

The latitude and longitude of two points are known, and the distance between two points is calculated. There are three ways to consult through the literature [27]–[29].

Method 1: The spherical cosine equation method. The method is theoretically applicable to the distance between any two points on the sphere. However, because there is a cos term in the equation, when the accuracy of the floating point operation of the system is not high, there is a large error in calculating the distance between two points that are closer.

Method 2: Cartesian coordinate system method. Because the method converts the spherical coordinates into rectangular coordinates and uses the Pythagorean theorem, it can only be used when the two points are close together. The higher the latitude, the narrower the range of use.

Method 3: Haversine method. This method is suitable for calculating the distance between any two points on the sphere. Using high school mathematics knowledge can prove that this method is a transformation of the spherical cosine function, because the cos term is replaced, so there is no problem of too much concern about the calculation accuracy of the system when calculating short distance.

In summary, we have chosen the third method to solve the distance(d) between two points. The following describes the method 3 in detail:

Solve d by giving $A(Aj, Aw)$, $B(Bj, Bw)$ and the mean radius of the earth R which is 6371 km.

Bring known quantities into the equation:

$$\begin{aligned} haver\sin(\frac{d}{R}) &= haver\sin(Bw - Aw) \\ &+ \cos(Aw)\cos(Bw)haver\sin(Aj - Bj), \end{aligned} \quad (18)$$

In the above equation:

$$haver\sin(\theta) = \sin^2(\frac{\theta}{2}) = \frac{1 - \cos(\theta)}{2}, \quad (19)$$

The solution shows that the distance we need is:

$$d = 2R\arctan\sqrt{\frac{h}{1 - h}}. \quad (20)$$

C. OVERALL COMMUNICATION

1) COMMUNICATION BETWEEN SHIP AND HOST

When the ship communicates with the host computer, it mainly uses the ship controller board communication protocol. Its uplink data format is 8 bytes per frame, as defined in Table 2. The downlink data format is 7 bytes per frame which is defined as Table 3.

In the above table, the different addresses represent different instructions, and the list of addresses and data we have defined is shown in Table 4:

2) COMMUNICATION BETWEEN SHIPS

In the actual navigation process, we adopt point-to-point communication in consideration of the real-time communication and packet loss problems. The MESH structure networks are used, and the networks are composed of a coordinator, a router, a terminal node. It features automatic dynamic route maintenance and can automatically find new routing paths. If the direct signal transmission from the sub ship to the main ship cannot be carried out during the ship's navigation, the node will automatically find a new path to transmit the information to the lead ship.

3) SHIP-SHORE COMMUNICATION

The USV terminal obtains the attitude information and position information of the ship in real time and forwards it

TABLE 2. Uplink data format.

Serial number	Name	Content	Length (bytes)
1	Frame header	0x5A	1
2	Address	(Reference address and data list)	1
3	Read/Write	0x01: Write, 0x00: Read	1
4	Data	(Corresponding address and data list)	2
5	Sum Check	Make the low bytes of the whole frame sum zero	1
6	Termination	$\langle CR\rangle \langle LF\rangle$	2

TABLE 3. Downlink data format.

Serial number	Name	Content	Length (bytes)
1	Frame header	0x5A	1
2	Address	(Reference address and data list)	1
3	Data	(Corresponding address and data list)	2
4	Sum Check	Make the low bytes of the whole frame sum zero	1
5	Termination	$\langle CR\rangle \langle LF\rangle$	2

TABLE 4. Address and data list.

Address number	Address definition	Operating	Parameter range	Boot default	Parameter unit
0x10	Power supply voltage	R	0-200	-	0.1V
0x11	Current consumption	R	0-100	-	0.1A
0x12	Charging current	R	0-100	-	0.1A
0x13	Water entering the cabin	RW	0-1023	-	Relative resistance decreases with water
0x20	Propulsion control	RW	0-1000	500	2 * (parameter value -500) $^{o}/_{oo}$
0x21	Steering gear control	RW	0-1000	500	2 * (parameter value -500) $^{o}/_{oo}$
0x30	Forward radar	R	0-500	-	1.7cm
0x40	Cabin drainage	RW	0-50	0	second
0x50 0x53	Logic Input Port, Channel 0-5V	R	High $= 1$, Low $= 0$	-	
0x60	Host Power Supply (Write 0 Suicide)	RW	Open $= 1$, Close $= 0$	1	
0x61 0x63	3 Channels 200mA, Leakage	RW	Open $= 1$, Close $= 0$	0	
0x80	Warning voltage	RW	0-200	0	0.1V
0x81	Stop voltage	RW	0-200	0	0.1V
0x82	Warning voltage(Too much suicide)	RW	0-200	0	0.1V
0x83	Power status	R	0-3	-	
0x84	Protects the current	RW	0-100	100	0.1A
0x85	current state	R	0-1	-	
0x8f	Transcendental enabling	RW	True $= 1$, False $= 0$	0	
0xF0	Self-test instruction	W	12345(10)	-	Trigger a self-check and return 12345 (10) after self-check
0xF1	Running time	R	0-32767	-	Number of minutes the system runs

to the ground control center through the B/S. The ground control center then disseminates the information to the lead USV through the B/S. The lead USV disseminates relevant information to the sub USV through the zigbee module point-to-point communication, which cooperates with the lead USV to perform automatic navigation after receiving the information from the ship. In this process, the ship's real-time heading, speed, location and other information are transmitted to the ground control center through the B/S for remote monitoring.

IV. USV SHIP COMPUTATIONAL MODEL

Ship computational models can be simply divided into linear computational models and nonlinear computational models. The linear ship computational model is simple and convenient to set up, but its accuracy is poor. Abkowitz's computational model of nonlinear ship motion is accurate, but it requires 67 parameters, and these parameters depend on ship model test or system identification technology, which is extremely difficult [30]. Considering this comprehensively, this paper uses the computational model of responsive nonlinear ship motion, which is actually a generalization of the linear Nomoto model. Firstly, on the basis of the classical Nomoto model, the effect of external factors such as wind, wave and current on the ship (which is given by the ship's attitude in the actual operation process) is added. At the same time, combined with PID algorithm, the computational model suitable for this kind of small underactuated unmanned ship is given. The model is explained in detail below.

A. CONSIDERING EXTERNAL FORCES

Adding nonlinearity to the ship's motion, according to the existing hardware conditions of our unmanned ships, the external force is measured by the horizontal drifting a_y and the yawing w_z measured by the nine-axis sensor. The linear equation of ship computational motion is expressed in matrix form:

$$\begin{bmatrix} \dot{v} \\ \dot{r} \end{bmatrix} = \begin{bmatrix} a_{11} & a_{12} \\ a_{21} & a_{22} \end{bmatrix} \begin{bmatrix} v \\ r \end{bmatrix} + \begin{bmatrix} b_{11} \\ b_{21} \end{bmatrix} \delta + \begin{bmatrix} c_{11} \\ c_{21} \end{bmatrix}, \quad (21)$$

In the above equation:

$$c_{11} = [L(I_{zz}{}' - N_{\dot{r}}{}')a_y + (Y_{\dot{r}}{}' - m'x_c{}')w_z]m'/S_1$$
$$c_{21} = [(N_{\dot{v}}{}' - m'x_c{}')a_y + (m' - Y_{\dot{v}}{}')w_z/L]m'/S_1. \quad (22)$$

We eliminate the v of the above matrix and get the equation of motion:

$$\psi''' - (a_{11} + a_{22})\psi'' - (a_{12}a_{21} - a_{11}a_{22})\psi' - (a_{21}c_{11} - a_{11}c_{21}) = b_{21}\delta' + (a_{21}b_{11} - a_{11}b_{21})\delta, \quad (23)$$

After the Laplace transform, the form of the transfer function is:

$$\psi(s) = \frac{K(1 + T_3 s)}{s(1 + T_1 s)(1 + T_2 s)}\delta(s) + \frac{T_1 T_2 T_8}{T_1 T_2 s^3 + (T_1 + T_2)s^2 + s}, \quad (24)$$

When $x \to 0$, there is $(1 - x) \approx 1/(1 + x)$, and the second and third order small quantities are ignored.

$$\psi = \frac{K}{s(Ts + 1)}\delta + \frac{T_6 T_8}{T_6 s^3 + T_7 s^2 + s}, \quad (25)$$

In the actual process, we use the heading angle to determine the deflection value of the ship's actual navigation rudder angle, so we resolve the above equation to:

$$\delta(s) = \frac{T}{K}s^2\psi(s) - \frac{1}{K}s\psi(s) - \frac{T_6 T_8(1 + Ts)}{K\left(T_6 s^2 + T_7 s + 1\right)}, \quad (26)$$

In the actual process, we need to use the time domain, so the above equation is solved as the time domain.

$$\delta(t) = \frac{T}{K}\psi''(t) - \frac{1}{K}\psi'(t) - \frac{T_6 T_8}{K T_3}e^{-\frac{1}{T_3}t}, \quad (27)$$

In the programming process, we use the discrete domain, and then we solve the problem by changing the time domain to the discrete domain:

$$\delta = \frac{T}{K}\left(\frac{\Delta_1 - 2\Delta_2 + \Delta_3}{\left(\frac{\Delta t_1 + \Delta t_2}{2}\right)^2}\right) - \frac{1}{K}\left(\frac{\Delta_1 - \Delta_3}{\Delta t_1 + \Delta t_2}\right) - \frac{T_6 T_8}{K T_3}e^{-\frac{1}{T_3}\left(\frac{\Delta t_1 + \Delta t_2}{2}\right)}, \quad (28)$$

In the above equation:

$$\Delta = \psi_1 - \psi_2, \quad (29)$$

where ψ_1, ψ_2 are the initial heading angle and actual measured heading angle. In the Eq.(4), the subscripts 1, 2, and 3 respectively indicate the current heading deviation, the heading deviation at the previous moment, and the heading deviation at the previous moment of the previous moment. Δt_1 indicates the time difference between the current time and the previous time. Δt_2indicates the time difference between the previous time and the previous time of previous time.

$$\begin{cases} K = (b_{11}a_{21} - b_{21}a_{11})/(a_{11}a_{22} - a_{12}a_{21}) \\ T_3 = b_{21}/(b_{11}a_{21} - b_{21}a_{11}) \\ T_6 = 1/(a_{11}a_{22} - a_{12}a_{21}) \\ T_7 = -(a_{11} + a_{22})/(a_{11}a_{22} - a_{12}a_{21}) \\ T_8 = a_{21}c_{11} - a_{11}c_{21} \\ T = T_7 - T_3. \end{cases} \quad (30)$$

B. COMBINING WITH PID ALGORITHM

In the application of the ship computational model to the actual process, it is found that the USV has a swaying phenomenon during the advancement process, considering that it may be due to its large adjustment coefficient. The PID controller has been in existence for nearly 70 years, and it has become one of the main technologies of industrial control because of its simple structure, good stability, reliable operation and convenient adjustment [31]. When the structure and parameters of the controlled object cannot be fully grasped, or the precise mathematical model is not obtained, other techniques of control theory are difficult to adopt [32], [33]. The structure and parameters of the system controller must be determined by experience and on-site debugging. At this time, it is most convenient to apply PID control technology.

When we do not fully understand a system and controlled objects, or can not obtain system parameters through effective measurement methods, it is most suitable to use PID control technology. Then we compare the incremental pid and finally give a ship computational model suitable for small USV.

The equation for the digital PID is [34]:

$$u(k) = K_p e(k) + K_i \sum_{j=0}^{k} e(j) + K_d[e(k) - e(k-1)]. \quad (31)$$

Then the equation of the incremental PID is:

$$\Delta u(k) = u(k) - u(k-1) = K_p[e(k) - e(k-1)] + K_i e(k) + K_d[e(k) - 2e(k-1) + e(k-2)]. \quad (32)$$

By comparing the above discrete equations, the theory plus external force and PID algorithm are combined to propose a new system model for small underactuated unmanned ships:

$$\delta = \frac{T}{K}\left(\frac{\Delta_1 - 2\Delta_2 + \Delta_3}{\left(\frac{\Delta t_1 + \Delta t_2}{2}\right)^2}\right) - \frac{1}{K}\left(\frac{\Delta_1 - \Delta_3}{\Delta t_1 + \Delta t_2}\right) - \frac{T_6 T_8}{K T_3}e^{-\frac{1}{T_3}\left(\frac{\Delta t_1 + \Delta t_2}{2}\right)} + K_i\Delta_1. \quad (33)$$

V. REAL SHIP VERIFICATION

A. THE EFFECT OF THE NEWLY PROPOSED SYSTEM MODEL ON THE REAL SHIP

1) USV BASIC PARAMETERS

First, the basic parameters of the USV are shown in TABLE 5.

TABLE 5. Address and data list.

Name	Numerical value	Name	Numerical value
Captain	1m	Breadth of ship	0.2m
Draft	0.043m	Drainage volume	$0.0042m^3$
Distance	0.038m	Rudder leaf area	$0.001938m^3$
Square coefficient	0.525		

2) CALCULATE THE ANGLE OF DEFLECTION OF THE RUDDER ANGLE

In the above, a ship computational model suitable for a small USV is mentioned. After re-combing, the steps of calculating the yawing angle in the actual process of the rudder angle are:

a. First use the parameters in TABLE 5 to calculate the dimensionless constant value of the ''two'' system.

b. Calculate 10 linear hydrodynamic derivatives.

c. Calculate the eight coefficients of the linear equation of ship maneuvering motion.

d. Calculate the six coefficients of the last proposed ship motion model.

e. According to the actual heading collected by the nine-axis sensor, bring the model into the actual adjusted rudder angle value.

3) PROBLEMS ENCOUNTERED DURING THE ACTUAL TEST OF THE SHIP

a: DATA MUTATION

When the USV initially starts, there is a sudden change in the data collected by the attitude sensor, resulting in a full rudder angle around the rudder angle, the ship is heavily surging, and the ship is unstable. Initially we considered to eliminate this mutation by delaying a certain amount of time, but the attitude sensor will only collect data after the actual interruption, which makes the delay useless.

Solution: In the actual operation process, by accumulating the number in the interruption, the propeller is not touched in the previous accumulation, and the data collected in the previous several times are discarded. This solves the surging phenomenon caused by signal mutation.

b: INFLUENCE OF EXTERNAL FACTORS

When we test the suitability of the ship computational model, we use heading control, which involves setting the initial heading angle. The initial heading angle of the ship at the beginning is the direction in which the ship is placed in the lake. Because of the flow of water, the heading at each moment will be biased. And we discard the first few states, which will result in inaccurate initial heading.

Solution: The data is collected for the first time after discarding, and the collected data is set to the initial value. The test chart in the lake is shown in Fig. 4. The green line in Fig. 5 is the heading dynamic map during the straight-line navigation.

In the two figures, according to the corrugation of Fig. 4, it can be seen that the ship travels in a straight line, and the green line in the route map of Fig. 5 is the actual heading of

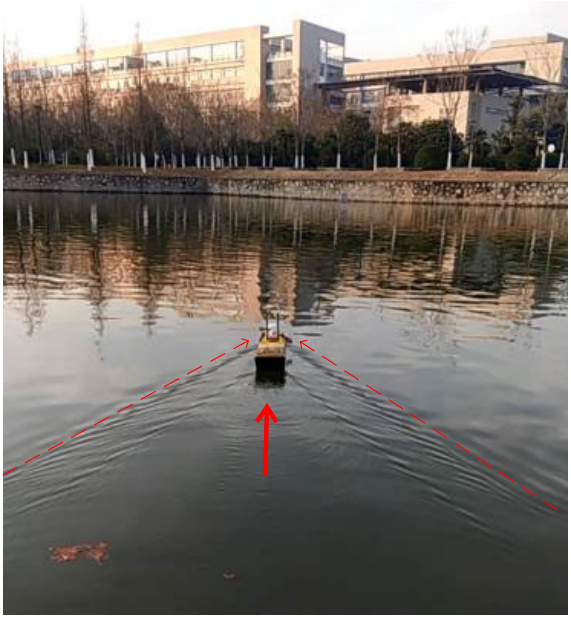

FIGURE 4. System model test diagram.

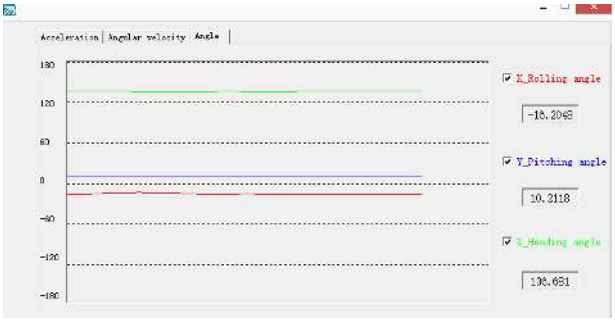

FIGURE 5. Straight line chart.

the ship. It can be seen from the straight line that its heading is almost stable during the course of the ship's heading, indicating that the proposed system model meets the experimental requirements in practice.

4) COMPARISON OF CONTROL EFFECTS

Fig. 6 shows the control effect of the improved computational model and the conventional Nomoto and Backstepping for stability. It can be seen from the comparison chart that the new ship computational model has a shorter time to return to the initial set heading angle of 134 degrees, and the overshoot is the smallest. It is the most stable. The red line is the effect diagram controlled by the Backstepping method. The method has a large overshoot, but the overall stability is better, but the constant adjustment parameter of the method has two values, and the parameter matching is troublesome during debugging. The Nomoto method of the green line, because it is linearly controlled, its oscillation is obvious and the system is not applicable.

In Fig. 7 and Fig. 8, the actual data simulation diagrams corresponding to the adjustment of the heading and rudder

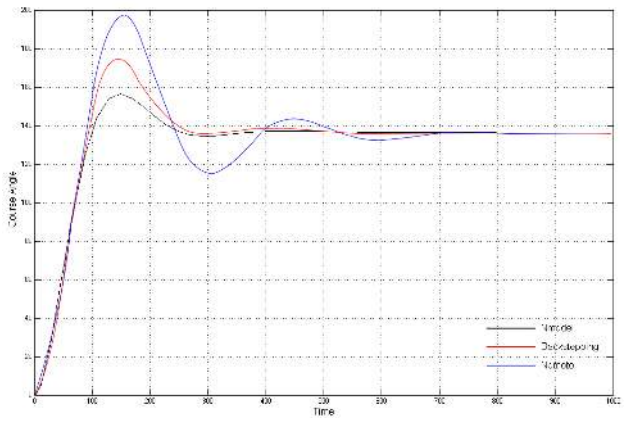

FIGURE 6. System control chart.

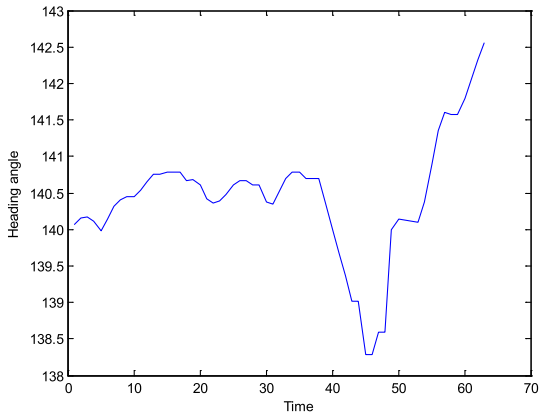

FIGURE 7. Heading angle.

angle are presented respectively during the movement of the ship. The actual heading is 140.5 degrees and the rudder angle 500 is positive for the rudder angle. The larger or smaller the rudder angle value is, the larger the rudder angle adjustment range is. By comparing the two figures, it can be seen that when the heading angle is small, the rudder angle value is reduced, indicating that the rudder angle is constantly adjusted when the heading angle is deviated, so that it can maintain the set heading.

In Fig. 8, it can be seen that the rudder angle is around 510 during the voyage. This is because the wind, wave and current has always been effective on the ship, so the ship gives the deflection value of the rudder angle in the current period according to its own model to make the ship run stably.

B. IMPLEMENTATION OF THE ANALYTIC HIERARCHY PROCESS

1) CONTROLLING THINKING

In order to highlight the situation of reaching the designated location, we set up to make the ship start a right-angle turn when it reaches the designated position, and then continue to move forward to verify.

First set a clock, start the right angle turn flag to 0, the ship follows the straight line. When it is detected that the ship

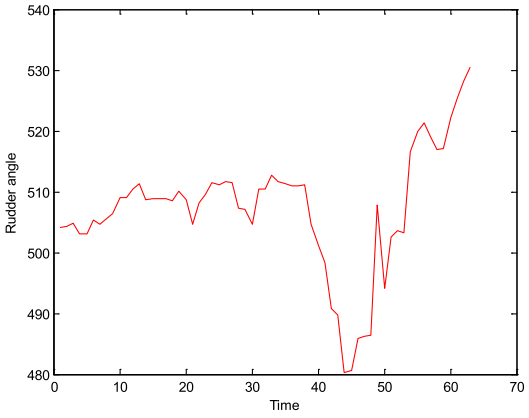

FIGURE 8. Rudder angle.

has reached the designated position, the right angle turn flag is 1, the steering gear is full, and the ship turns. When it is detected that the difference between the heading angle and the set heading angle is 90°(87°- 93°), the right angle turning flag is 0, and the heading angle at this moment is set to the initial heading angle (the setting heading angle), the unmanned boat continues straight ahead.

2) PROBLEMS ENCOUNTERED AND SOLUTIONS

a: SOLUTION TO HEADING ANGLE DEVIATION

The heading angle is a value given by $-180°$ and $180°$, which is equivalent to a circle. If it is simply expressed by the following equation, the value sought cannot represent the difference of the actual angle.

$$\Delta\psi = \psi_1 - \psi_2. \tag{34}$$

where ψ_1, ψ_2 are the initial heading angle and actual measured heading angle.

For example, if the heading angle is set to 130°and the actual heading angle is $-150°$, then using the above equation, the heading deviation $= 280°$, the actual difference should be $-80°$(the counterclockwise is positive)

Solution:

a. The heading deviation value is 180∼360°, then the actual heading deviation value needs to be subtracted by 360°.

b. The heading deviation value is $-360 \sim -180°$, then the actual heading deviation value needs to be added by 360°.

c. The general situation is Eq.(34).

b: THE PROBLEM THAT MAY BE ENCOUNTERED DURING THE VOYAGE IS THE PROBLEM OF DEVIATION FROM THE TRACK

Solution: During the course of running, nine axes have been collecting ship motion data, through the course value, to observe whether or not yaw. In case of yaw, the distance between the actual ship and the set point is calculated, and if the distance increases, the corresponding adjustment (the model of the call system, the rudder angle of the ship is adjusted accordingly) is made until the designated point is reached.

FIGURE 9. Turn around at a certain point.

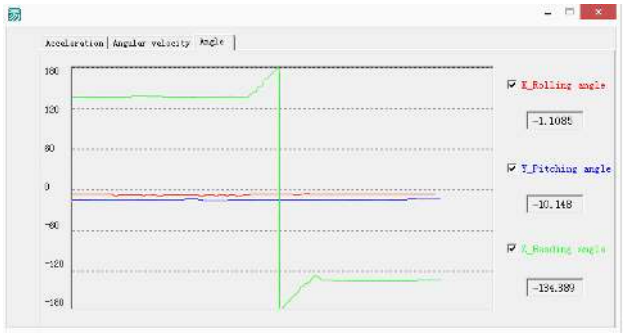

FIGURE 10. Turning heading graph.

3) ACTUAL CONTROL EFFECT

Fig. 9 is the actual chart of fixed-point turning, and Fig. 10 is the chart of turning course. From the water wave of Fig. 9, it can be seen that the state of the ship is almost 90°after the start of the turn. In the green line in Fig. 10, it can be seen that the heading is always around 135°, indicating that the ship has been doing a linear motion and reaching the designated position to start the turn. After turning, the heading is stable at - 140°, and the difference is about 85 °, which means that it has basically reached the designated position and realized right-angle turning.

Fig. 11 is the latitude and longitude data graph. It can be seen that we first reach a certain point and then make a right-angle turn.

C. COMMUNICATION EXPERIMENT

1) SHIP COMMUNICATION EXPERIMENT

Considering its real-time and packet loss issues, we use P2P communication in the communication between ships. According to Zigbee's automatic routing function, in the arrangement, we placed the coordinator on the lead USV, placed the terminal node on the sub USV, and arranged the router nearby. This prevents the path from the lead USV

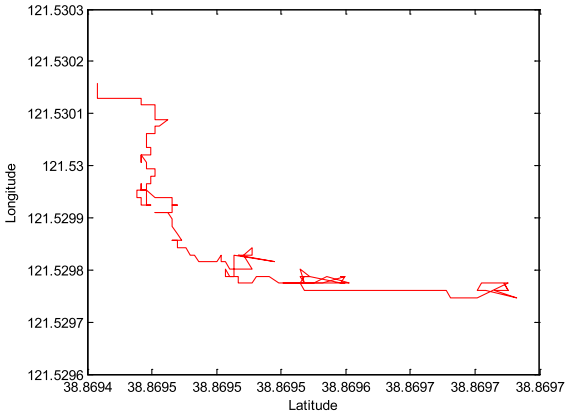

FIGURE 11. Latitude and Latitude data map graph.

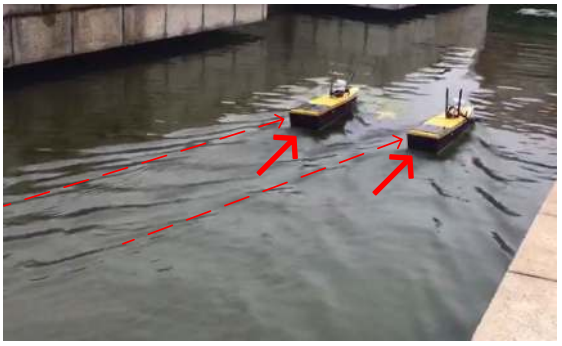

FIGURE 12. Collaborative straight line forward.

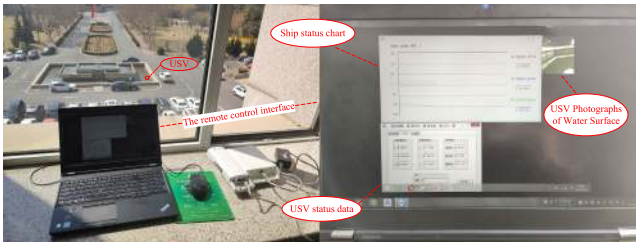

FIGURE 13. Collaborative straight line forward.

to the sub USV from being destroyed, and a route can be automatically routed so that the two USVs can continue to communicate. The actual control effect is shown in Fig. 12.

In Fig. 12, the lead USV (left) sends a command for straight-line navigation to the sub USV (right), and the command is received from the sub USV to cooperate with the lead USV.

2) GROUND CONTROL CENTER AND SHIP COMMUNICATION

In the ship and ground control center, we use the bridge and B/S architecture to achieve remote control. The actual control is shown in Fig. 13. Fig. 14 shows the control interface on the webpage.

In Fig. 13, there are ships in operation in the pool at the bottom of the left, and in the right, there is a remote operation interface. The lead USV information is given by the

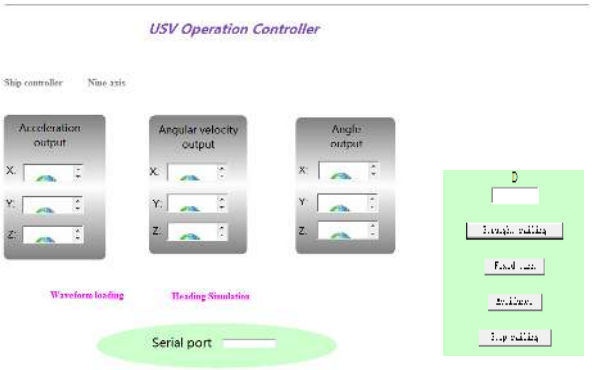

FIGURE 14. Web control interface.

computer and then the lead USV performs the corresponding movement.

In Fig. 14, this interface is a display interface that can be seen at the remote end of the B/S architecture. Click on the motion, the green box in the lower right corner will pop up. Click on the straight line to sail, the information is disseminate to the USV through the B/S, the lead USV is disseminate to the corresponding command by the ZigBee, and then the two ships work together.

VI. CONCLUSION

Facing the future ocean, aiming at the scenarios of ocean communication networking and maritime transportation, this paper designs an integrated Space-Air-Ground-Sea communication control system based on mobile computing technology to solve a series of practical problems such as information coverage at sea, searching and positioning. The small USV is the backbone of the entire system among them. First, we use a variety of sensors to sense the location of container and collect ship information. Secondly, we model the system of a small USV with the help of the classic Nomoto model. On this basis, full consideration is given to the disturbance of the ship by external factors such as the wind, wave and current in the actual voyage. Combined with the PID control algorithm, a computational model suitable for this type of USV is established. In addition, zigbee point-to-point communication is used to realize real-time communication between multiple USV, and a basic networking structure is conducted, which is based on multiple USV, covered satellites, drones, underwater sensors and other devices. Finally, we use B/S architecture to realize the information dissemination and control instruction decoupling, and remotely monitor the USV. The linkage with the position information of the falling water container collected by the underwater sensor is realized, and the container search and rescue work is completed. In the future work, we will continue to study how to send the video captured by the unmanned ship clearly to the ground control terminal.

REFERENCES

[1] J. Zheng, F. Meng, and Y. Li, "Design and experimental testing of a free-running ship motion control platform," *IEEE Access*, vol. 6, pp. 4690–4696, 2018.

[2] B. Winden, S. R. Turnock, and D. A. Hudson, "Self-propulsion modelling of the KCS container ship using an open source framework," in *Proc. Numer. Towing Tank Symp.*, 2014, pp. 199–205.

[3] Z. Dong, T. Bao, M. Zheng, X. Yang, L. Song, and Y. Mao, "Heading control of unmanned marine vehicles based on an improved robust adaptive fuzzy neural network control algorithm," *IEEE Access*, vol. 7, pp. 9704–9713, 2019.

[4] S. Fish and A. Sitzman, "Unmanned vehicles for mobile electromagnetic launch platforms," *IEEE Trans. Magn.*, vol. 45, no. 1, pp. 639–640, Jan. 2009.

[5] Y. He, S.-Y. He, Y.-H. Zhang, G.-J. Wen, D.-F. Yu, and G.-Q. Zhu, "A forward approach to establish parametric scattering center models for known complex radar targets applied to SAR ATR," *IEEE Trans. Antennas Propag.*, vol. 62, no. 12, pp. 6192–6205, 2014.

[6] O. A. Yakimenko, I. I. Kaminer, W. J. Lentz, and P. A. Ghyzel, "Unmanned aircraft navigation for shipboard landing using infrared vision," *IEEE Trans. Aerosp. Electron. Syst.*, vol. 38, no. 4, pp. 1181–1200, Oct. 2002.

[7] X. Liu, "Node deployment based on extra path creation for wireless sensor networks on mountain roads," *IEEE Commun. Lett.*, vol. 21, no. 11, pp. 2376–2379, Nov. 2017.

[8] Z. Peng, J. Wang, and J. Wang, "Constrained control of autonomous underwater vehicles based on command optimization and disturbance estimation," *IEEE Trans. Ind. Electron.*, vol. 66, no. 5, pp. 3627–3635, May 2019.

[9] Y. Shi, C. Shen, H. Fang, and H. Li, "Advanced control in marine mechatronic systems: A survey," *IEEE/ASME Trans. Mechatronics*, vol. 22, no. 3, pp. 1121–1131, Jun. 2017.

[10] D. Maalouf, A. Chemori, and V. Creuze, "Adaptive depth and pitch control of an underwater vehicle with real-time experiments," *Ocean Eng.*, vol. 98, pp. 66–77, Apr. 2015.

[11] T. Gao, S. Yin, H. Gao, X. Yang, J. Qiu, and O. Kaynak, "A locally weighted project regression approach-aided nonlinear constrained tracking control," *IEEE Trans. Neural Netw. Learn. Syst.*, vol. 29, no. 12, pp. 5870–5879, Dec. 2018.

[12] T. H. Bryne, J. M. Hansen, R. H. Rogne, N. Sokolova, T. I. Fossen, and T. A. Johansen, "Nonlinear observers for integrated INS/GNSS navigation: Implementation aspects," *IEEE Control Syst. Mag.*, vol. 37, no. 3, pp. 59–86, Jun. 2017.

[13] Y. Wang, S. Wang, and M. Tan, "Path generation of autonomous approach to a moving ship for unmanned vehicles," *IEEE Trans. Ind. Electron.*, vol. 62, no. 9, pp. 5619–5629, Sep. 2015.

[14] W. Zhang, W. Liu, T. Wang, A. Liu, Z. Zeng, H. Song, and S. Zhang, "Adaption resizing communication buffer to maximize lifetime and reduce delay for WVSNs," *IEEE Access*, vol. 7, pp. 48266–48287, 2019.

[15] K. H. Ang, G. Chong, and Y. Li, "PID control system analysis, design, and technology," *IEEE Trans. Control Syst. Technol.*, vol. 13, no. 4, pp. 559–576, Jul. 2005.

[16] J. Y. Lee, M. Jin, and P. H. Chang, "Variable PID gain tuning method using backstepping control with time-delay estimation and nonlinear damping," *IEEE Trans. Ind. Electron.*, vol. 61, no. 12, pp. 6975–6985, Dec. 2014.

[17] Z. Pan, F. Dong, J. Zhao, L. Wang, H. Wang, and Y. Feng, "Combined resonant controller and two-degree-of-freedom PID controller for PMSLM current harmonics suppression," *IEEE Trans. Ind. Electron.*, vol. 65, no. 9, pp. 7558–7568, Sep. 2018.

[18] Z. Liu, "Ship adaptive course keeping control with nonlinear disturbance observer," *IEEE Access*, vol. 5, pp. 17567–17575, 2017.

[19] A. Fujimura, A. Soloviev, and V. Kudryavtsev, "Numerical simulation of the wind-stress effect on SAR imagery of far wakes of ships," *IEEE Geosci. Remote Sens. Lett.*, vol. 7, no. 4, pp. 646–649, Oct. 2010.

[20] J. Du, C. Guo, S. Yu, and Y. Zhao, "Adaptive autopilot design of time-varying uncertain ships with completely unknown control coefficient," *IEEE J. Ocean. Eng.*, vol. 32, no. 2, pp. 346–352, Apr. 2007.

[21] J. Wang, H. Zhou, Y. Li, Q. Sun, Y. Wu, S. Jin, T. Q. S. Quek, and C. Xu, "Wireless channel models for maritime communications," *IEEE Access*, vol. 6, pp. 68070–68088, Dec. 2018.

[22] L. Chi, Y. Qi, Z. Weng, W. Yu, and W. Zhuang, "A compact wideband slot-loop directional antenna for marine communication applications," *IEEE Trans. Veh. Technol.*, vol. 68, no. 3, pp. 2401–2412, Mar. 2019.

[23] H.-X. Wu, S.-K. Cheng, and S.-M. Cui, "Communication of vehicle management unit in the electric vehicle," *IEEE Trans. Magn.*, vol. 41, no. 1, pp. 514–517, Jan. 2005.

[24] X. Liu and P. Zhang, "Data drainage: A novel load balancing strategy for wireless sensor networks," *IEEE Commun. Lett.*, vol. 22, no. 1, pp. 125–128, Jan. 2018.

[25] R. He, A. F. Molisch, F. Tufvesson, Z. Zhong, B. Ai, and T. Zhang, "Vehicle-to-vehicle propagation models with large vehicle obstructions," *IEEE Trans. Intell. Transp. Syst.*, vol. 15, no. 5, pp. 2237–2248, Oct. 2014.
[26] W.-Y. Shieh, C.-C. J. Hsu, C.-H. Lin, and T.-H. Wang, "Investigation of vehicle positioning by infrared signal-direction discrimination for short-range vehicle-to-vehicle communications," *IEEE Trans. Veh. Technol.*, vol. 67, no. 12, pp. 11563–11574, Dec. 2018.
[27] L. Du and H. Dao, "Information dissemination delay in vehicle-to-vehicle communication networks in a traffic stream," *IEEE Trans. Intell. Transp. Syst.*, vol. 16, no. 1, pp. 66–80, Feb. 2015.
[28] C. Joo and J. Choi, "Low-delay broadband satellite communications with high-altitude unmanned aerial vehicles," *J. Commun. Netw.*, vol. 20, no. 1, pp. 102–108, Feb. 2018.
[29] H. Jiang, Z. Zhang, J. Dang, and L. Wu, "A novel 3-D massive MIMO channel model for vehicle-to-vehicle communication environments," *IEEE Trans. Commun.*, vol. 66, no. 1, pp. 79–90, Jan. 2018.
[30] N. Nakamura, H. Tsunomachi, and R. Fukui, "Road vehicle communication system for vehicle control using leaky coaxial cable," *IEEE Commun. Mag.*, vol. 34, no. 10, pp. 84–89, Oct. 1996.
[31] Y. Zhao, Z. Li, B. Hao, P. Wan, and L. Wang, "How to select the best sensors for TDOA and TDOA/AOA localization?" *China Commun.*, vol. 16, no. 2, pp. 134–145, Feb. 2019.
[32] H. Xiong, Z. Chen, B. Yang, and R. Ni, "TDOA localization algorithm with compensation of clock offset for wireless sensor networks," *China Commun.*, vol. 12, no. 10, pp. 193–201, Oct. 2015.
[33] Y. Liu, A. Liu, X. Liu, and X. Huang, "A statistical approach to participant selection in location-based social networks for offline event marketing," *Inf. Sci.*, vol. 480, pp. 90–108, Apr. 2019.
[34] J. Tan, W. Liu, M. Xie, H. Song, A. Liu, M. Zhao, and G. Zhang, "A low redundancy data collection scheme to maximize lifetime using matrix completion technique," *EURASIP J. Wireless Commun. Netw.*, vol. 2019, no. 1, p. 5, 2019. doi: 10.1186/s13638-018-1313-0.

TINGTING YANG (M'13) received the B.Sc. and Ph.D. degrees from Dalian Maritime University, China, in 2004 and 2010, respectively. She is currently an Associate Professor with the School of Electrical Engineering and Intelligentization, Dongguan University of Technology, China. Since September 2012, she has been a Visiting Scholar with the Broadband Communications Research (BBCR) Lab, Department of Electrical and Computer Engineering, University of Waterloo, Canada. Her research interests include maritime wideband communication networks, DTN networks, and green wireless communication. She serves as a TPC Member for IEEE ICC'14 and ICC'15 Conference. She also serves as the Associate Editor-in-Chief for the *IET Communications*, and an Advisory Editor for *SpringerPlus*.

YUEJUN GUO received the B.S. degree in the Internet of Things from Dalian University, China, in 2017. She is currently pursuing the M.S. degree with the Navigation College, Dalian Maritime University, China. Her research interests include USV system modeling, ship motion control, clustering protocols, and maritime broadband communication networks.

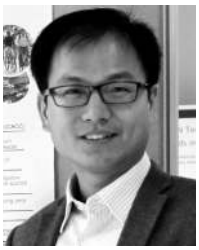

YI ZHOU (M'15) received the B.S. degree in electronic engineering from the First Aeronautic Institute of Air Force, China, in 2002, and the Ph.D. degree in control system and theory from Tongji University, China, in 2011. From 2002 to 2005, he was a Research and Development Engineer with Beijing Centergate Technologies Company Ltd., China. He was a Visiting Researcher with the Telecommunications Research Center (ftw.), Vienna, Austria, in 2009, and the National Institute of Informatics, Tokyo, Japan, in 2010. From 2014 to 2015, he was a Postdoctoral Fellow with the University of Waterloo, Waterloo, ON, Canada. He is currently an Associate Professor with the School of Computer and Information Engineering, Henan University, Kaifeng, China. He is also the Director of the International Joint Research Laboratory for Cooperative Vehicular Networks, Henan, China. He also leads the Vehicular Networking Institute of Central Plains Silicon Valley. His research interests include vehicular cyber-physical systems and multi-agent design for vehicular networks.

SIWEN WEI received the B.S. degree in measurement and control technology and instrumentation from Dalian Maritime University, China, in 2017. She is currently pursuing the M.S. degree with the Navigation College, Dalian Maritime University, China. Her research interests include ship motion control, cognitive radio networks, and maritime wideband communication networks.